

MICROSTRUCTURE AND WEAR PROPERTY OF IN-SITU OXIDE REINFORCED CrMnFeCoNi HIGH ENTROPY ALLOY COMPOSITE FABRICATED BY SELECTIVE LASER MELTING

CrMnFeCoNi high entropy alloy (HEA) which had nano oxide particles formed during additive manufacturing process was fabricated using a selective laser melting (SLM) process (hereinafter SLM Cantor HEA). The microstructure of the fabricated SLM Cantor HEA and the wear properties according to the applied load (5 N, 15 N) were investigated. SLM Cantor HEA was consist of nano-size oxides and high dislocation density, resulting in superior hardness compared to conventional processed CrMnFeCoNi HEA. As a result of the wear test, it showed abrasive and oxidative wear behavior regardless of applied load. But in case of 15 N load condition, it showed more finer worn microstructure with increased wear load, and had a contradictory effect on each friction coefficient and wear rate. Based on the above results, the wear mechanism of in-situ oxide reinforced SLM Cantor HEA was discussed in relation with the microstructure.

Keywords: Selective laser melting; CrMnFeCoNi High entropy alloy; in-situ formed oxide; Wear; Microstructure

1. Introduction

High entropy alloy (HEA) is a new concept alloy designed for multiple (5 or more) principal elements to have almost equal elemental ratios, unlike the typical alloy development paradigm in which trace amounts of alloying elements are added to one or two principal elements. HEA can exhibit excellent fracture toughness, hydrogen embrittlement resistance, and oxidation resistance due to severe lattice distortion effect and sluggish diffusion and is expected to be a next-generation structural material [1-3].

Equiatomic CrMnFeCoNi HEA (Cantor HEA), one of the representative HEAs, is known to maintain a stable FCC single phase at 800°C or below and exhibit excellent room-temperature and cryogenic toughness due to twinning induced plasticity (TWIP) generated by low stacking fault energy [3,4]. However, as it still shows low yield strength to be applied as a structural material, many efforts are being made to improve it, such as particle reinforcement and ultra-refinement of grain size [5,6].

In previous studies, authors have proposed utilizing the properties of the selective laser melting (SLM) process, one of the additive manufacturing techniques, as an effective way

to fabricate HEA-based composites [7-10]. When applying the SLM process through previous research results, it was possible to manufacture in-situ formed particle composites that form reinforced particles during the process through the interstitial element (C, O, etc.) control without using a powder with pre-mixed reinforced particles, and improvements in mechanical properties, such as tensile strength, high-temperature mechanical properties, and hydrogen embrittlement resistance were confirmed [11-14].

Furthermore, HEA is expected to be applied as a structural material related to safety due to its excellent chemical resistance, radiation resistance, and hydrogen embrittlement resistance, and thus verification of additional mechanical properties is necessary [14-16]. In particular, wear is the type that causes most part loss in everyday life, and wear loss is directly related to fatigue failure and can cause part damage [15,16]. However, there are currently no research results on the wear behavior of SLM-built CrMnFeCoNi (SLM Cantor HEA).

In this study, we intended to investigate the wear properties of SLM Cantor HEA composite with additional in-situ oxides manufactured through the atmosphere control of the SLM process and identify the wear behavior by linking microstructures before and after wear.

¹ INHA UNIVERSITY, DEPARTMENT OF MATERIALS SCIENCE AND ENGINEERING, INCHEON, KOREA

* Corresponding author: keeahn@inha.ac.kr



2. Experimental

Equiatomic Cantor HEA powders used as feedstock for the SLM process were fabricated utilizing a gas atomization process. Powders showed spherical morphology and size distribution of $d_{10} = 17.9 \mu\text{m}$, $d_{50} = 26.1 \mu\text{m}$, and $d_{90} = 38.2 \mu\text{m}$. The results of chemical composition analysis of the powder using X-ray fluorescence (XRF, Axios, Malvern Panalytical, U.K.) showed an almost equiatomic composition with 20.47 at.% Co, 19.28 at.% Cr, 20.16 at.% Fe, 19.08 at.% Mn and 21.01 at.% Ni.

Mlab Cusing (Concept Laser GmbH, Germany) equipment was used for the SLM process, and Ar gas was used as the atmosphere. Optimal conditions (scanning speed: 600 mm/s, hatch spacing: 80 μm , build thickness: 25 μm , laser power: 90 W, and focal spot size: 50 μm) selected through pre-tests were applied to the process parameters with a low porosity of 0.13%. Materials were manufactured with bar-type dimensions of 85 mm \times 10 mm \times 10 mm, and the scanning pattern applied a zig-zag mode rotated at 45° with the longitudinal direction of the specimen for each layer, and the scanning direction with neighboring layer had a relationship of 180°.

The final mirror polishing was first performed with \sim #4000 grit SiC paper and 0.04 μm silica colloidal suspension

to examine microstructures initial and after wear tests of SLM Cantor HEA. Backscattered electron (BSE) imaging used field emission scanning electron microscopy (FE-SEM, MYRA 3 XMH, Tescan, Czech Republic), and chemical composition analysis used an energy dispersive X-ray spectrometer (EDS, Mmax 50, Oxford, U.K.). Electron back scattered diffraction (EBSD, Nordlys-CMOS detector, Oxford, U.K.) analysis was used to obtain additional crystallographic information.

A room-temperature Vickers test was performed to confirm the basic mechanical properties of the material surface. The indentation load was 0.3 kgf, the test time was 10 sec, and the test was repeated 20 times, and the average value was used as the representative value. The specimen was cut into a dimension of 10 mm \times 10 mm \times 10 mm for wear test, the SD plane (parallel to building direction (BD)) was designated as the wear surface, and the surface was ground with \sim #4000 grit SiC paper to evaluate wear properties. In the case of the ball-on disk wear test performed at room temperature, an alumina ball with a diameter of 6 mm was used as a counterpart material, and the conditions for sliding radius: 4 mm, total sliding distance: 500 m, and linear speed: 0.1 m/s were applied. At the same time, two conditions of loaded force (5 N and 15 N) were applied to investigate wear properties according to wear load, and each wear specimen was named 5 N and 15 N.

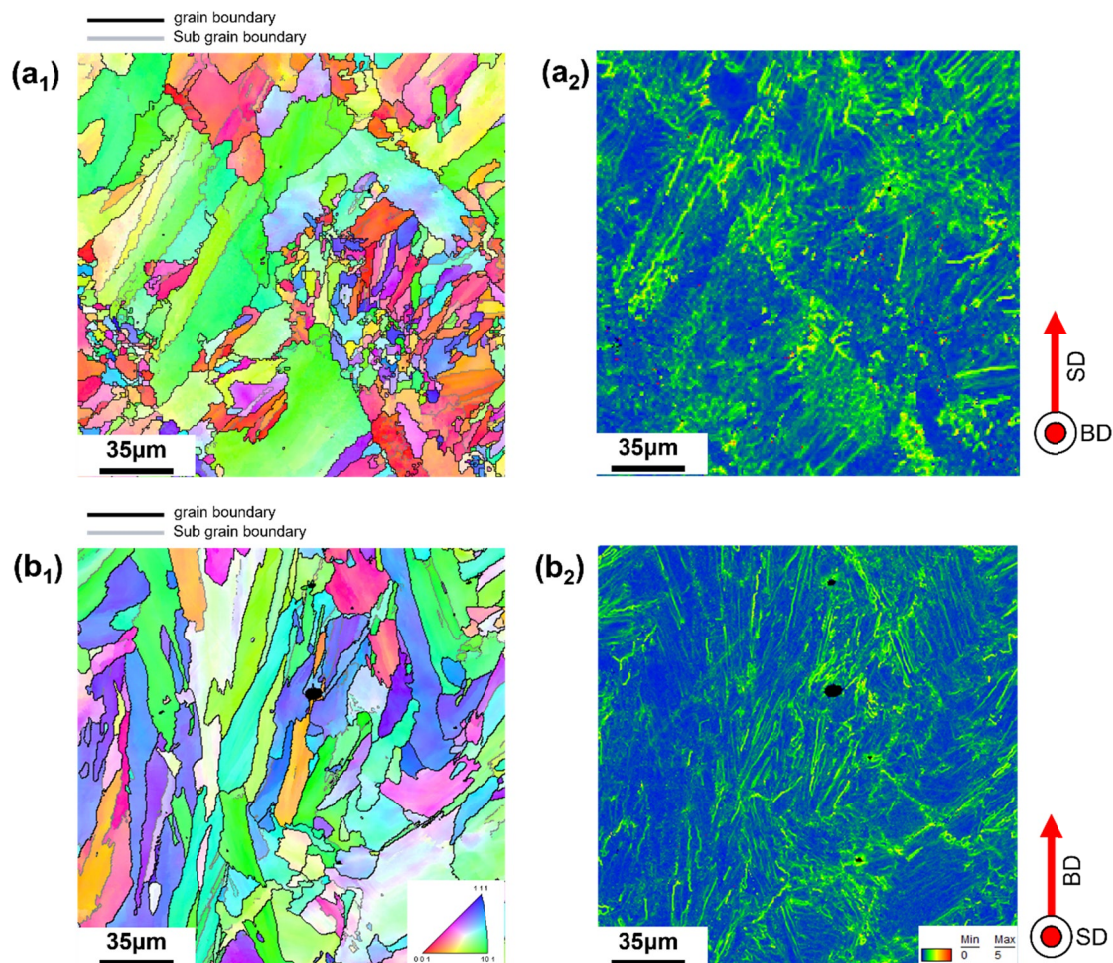


Fig. 1. EBSD analysis results of initial microstructure of the SLM Cantor HEA; (a₁), (b₁) IPF maps and (a₂), (b₂) KAM maps on (a) BD plane and (b) SD plane

3. Results and discussions

Fig. 1 shows the EBSD analysis results of the initial microstructure of the SLM Cantor HEA. The average grain size analyzed was $11.75\ \mu\text{m}$, and the area spanning the line irradiated by the laser was relatively composed of refined grains. Grains also showed epitaxial grains along the BD under the influence of laser sources and intense heat flux [17]. The grain contained sub-grains with a 10° or less misorientation angle. Metals manufactured by the SLM process can generally have many sub-structures [10-14, 18]. The observation of the BSE-SEM image (Fig. 2) showed fine sub-cells of 1 to $2\ \mu\text{m}$ inside the grain, and secondary phases were present on the cell boundaries. These second phases were suggested to be Mn_2O_3 in a previous study and the volume fraction of the particle was calculated about 0.54 vol.% [8]. Also, the cells were decorated with dislocation networks and oxides. Mn_2O_3 in SLM Cantor HEA is an in-situ oxide formed by pressure generated by an intense laser and Marangoni flux during the SLM process. They are fine oxides synthesized by oxygen in the SLM equipment chamber environment penetrating into the melt pool by the laser pressure and reacting with the alloying element [19]. Efforts have been

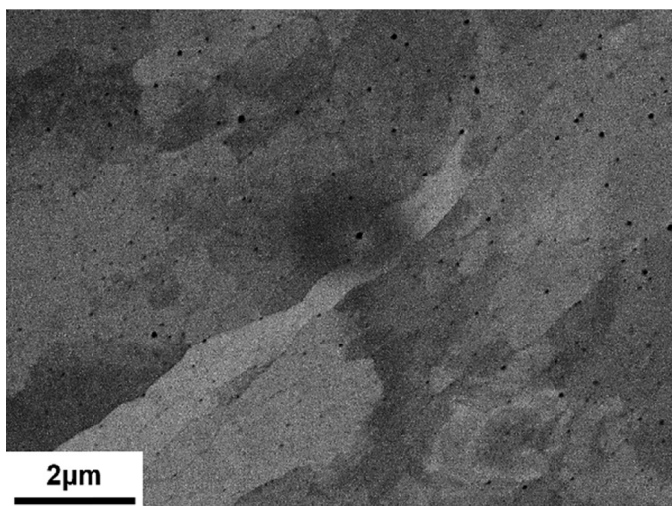


Fig. 2. Representative BSE-SEM image showing sub-cell structure and in-situ formed Mn_2O_3

made to manufacture composite materials or fine-grain alloys involving complex thermomechanical procedures to improve the strength of HEA [5,6]. However, when applying the SLM process, SLM is expected to be used as an efficient manufacturing technology for high-strength alloys because it is possible to manufacture alloys with nanoparticles and high inner stress by controlling impurity atoms or atmosphere.

We measured the Vickers hardness to investigate the surface mechanical properties of SLM Cantor HEA and obtained an average hardness value of $298.13 \pm 13.21\ \text{HV}$ (SD plane) and $276.56 \pm 15.17\ \text{HV}$ (BD plane). The alloy showed mechanical anisotropy, which can be caused by that the average grain size of the SD plane is slightly finer. In contrast, the hardness of equiatomic Cantor HEAs manufactured by a conventional process is reported to be between 150 and 230 HV [20,21]. SLM Cantor HEA can be described as having much higher hardness properties than typical processed Cantor due to the reinforcing effect of high dislocation density, nanoparticles, etc.

Fig. 3 shows the wear test results of SLM Cantor HEA. As a result of the wear test according to the wear load, the weight loss due to wearing was 0.0146 g in the case of 5 N and 0.0167 g in the case of 15 N. Despite the three-fold increase in the load, the difference in the amount of wear loss increased slightly by 0.0021 g. The sliding distance versus coefficient of friction (COF) curve showed different characteristics depending on the load. The COF of 5 N was generally lower than that of 15 N, and a steady state was maintained after the initial static friction step. On the other hand, in the case of 15 N, the gradual decrease and increase of COF were repeated, and the fluctuation of the COF curve was found in the re-increase section. The curve fluctuations are a sign of intermittent stick-slip wear and are reported to be caused by interactions between the counterpart and the worn materials' surfaces. They can also be caused by various factors, such as adhesion, delamination, and roughness [22-24]. Calculating the specific wear rate according to the load (Fig. 3) showed that the wear rate decreased as the load increased. Moreover, compared to Cantor manufactured using a casting process ($0.30 \times 10^{-3}\ \text{mm}^3/\text{N m}$), 15 N showed a slightly better wear resistance, i.e., a lower wear rate [25]. Ductile metals generally show better wear resistance at high loads when showing high

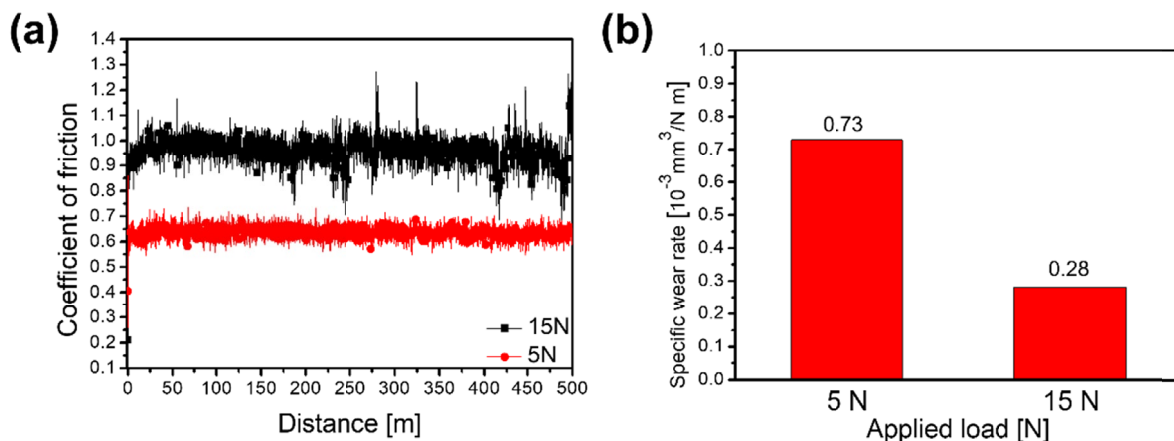


Fig. 3. Results of wear test; (a) coefficient of friction versus wear distance and (b) specific wear rate versus applied load

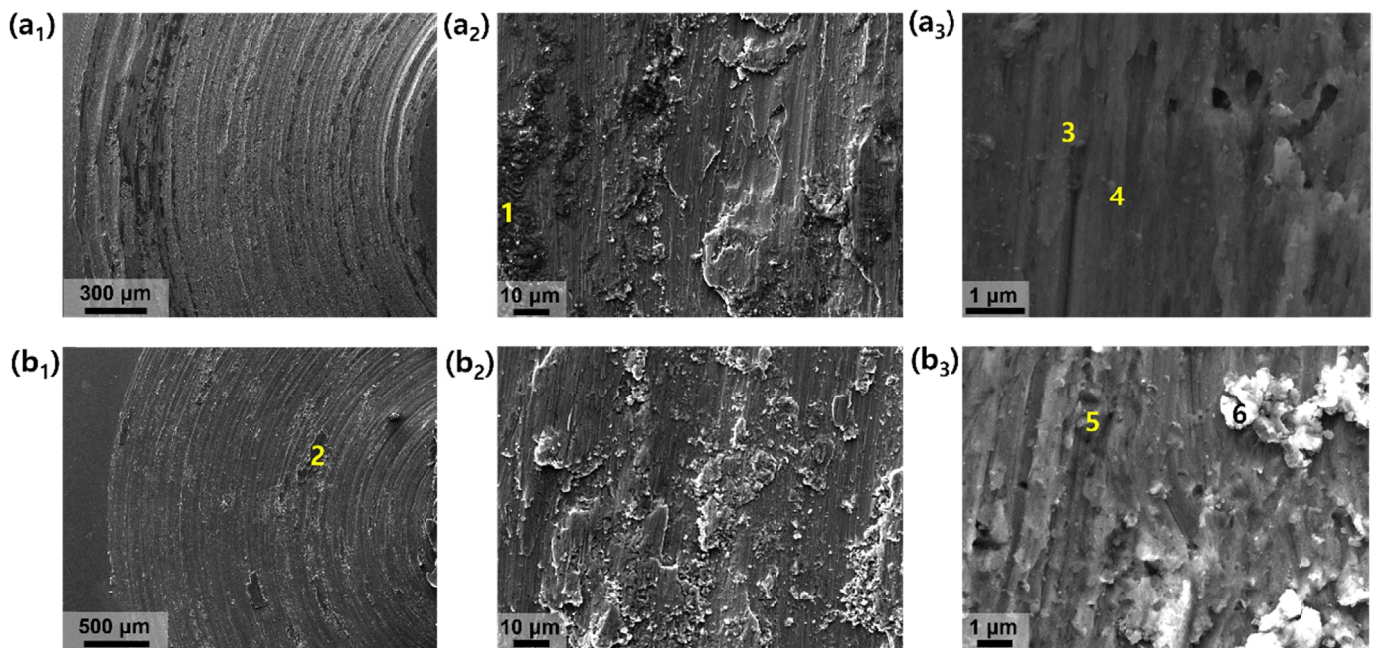
hardness, and SLM Cantor HEA can be understood as having better hardness and wear resistance due to finer microstructures and in-situ oxides [26].

We observed the friction surface to analyze the wear behavior closely, and the results are shown in Fig. 4. Many grooved scratches parallel to the sliding direction were commonly observed on the worn surface at 5 N and 15 N, suggesting an abrasive wear behavior [27]. In addition, the overall oxygen content on the wear surface increased, inferring the oxidative wear behavior. There was more debris (3 to 6 on the Fig. 4) on the surface of 15 N worn surface than 5 N, and the EDS analysis confirmed that these debris were Al_2O_3 fragments (6), which were counterpart, oxides or detached matrix. Showing a lower COF at 5 N is considered to be related to the oxides coverage of the alloy surface [20,22]. Observation of the specimen's cross-sectional microstructure after wear (Fig. 5) showed severe plastic deformation in the region directly below the worn surface in both the 5 N and 15 N wear conditions and a nanocrystalline layer on the worn surface. However, plastic deformation was observed in a wider area due to a higher load in the case of 15 N, and the microstructures on the worn surface layer were finer than that of 5 N. Higher loads may impart more deformation below the worn surface, and they can form a high gradient of strain between the area directly below the worn surface and

the region below it [25,28]. Also, the sliding duration increases as the contact area between the indenter and the worn surface increases, which it is expected to cause more deformation. Accordingly, the increase in strain rate and strain causes severe deformation and promotes grain refinement by partitioning and crossing between multiple slip bands and the microband interaction [20]. Therefore, surface strengthening due to grain refinement is suspected in the case of the 15 N wear load condition, and it is determined that the lower wear rate was caused by the self-lubricant effect of the detached ultra-fine equiaxed grains present in the debris [27]. This dry solid lubrication may help to reduce COF with increased wear distance, and can also be understood as showing an overall trend of decreasing COF of 15 N conditions in Fig. 3(a) [22].

4. Conclusions

In this study, we investigated the wear properties according to the applied load of in-situ oxide Cantor HEA composite manufactured by the SLM process and analyzed the wear behavior in connection with microstructure. The manufactured SLM Cantor HEA consisted of nano-sized Mn_2O_3 and main in a sub-structure decorated with Mn_2O_3 and a dislocation network.



(Wt.%)	1	2	3	4	5	6
O	29.25	31.45	9.70	4.46	2.72	9.88
Al	0.63	13.38	0.20	0.05	0	8.55
Co	14.63	10.97	18.68	19.32	20.9	17.75
Cr	14.09	11.25	17.71	18.23	18.67	16.03
Fe	13.50	11.16	17.99	18.84	19.24	16.33
Mn	13.52	10.73	16.82	19.35	17.95	15.56
Ni	14.38	11.06	18.90	19.75	20.52	15.90

Fig. 4. SEM observation results with EDS showing worn out surfaces; (a) 5 N and (b) 15 N wear load conditions

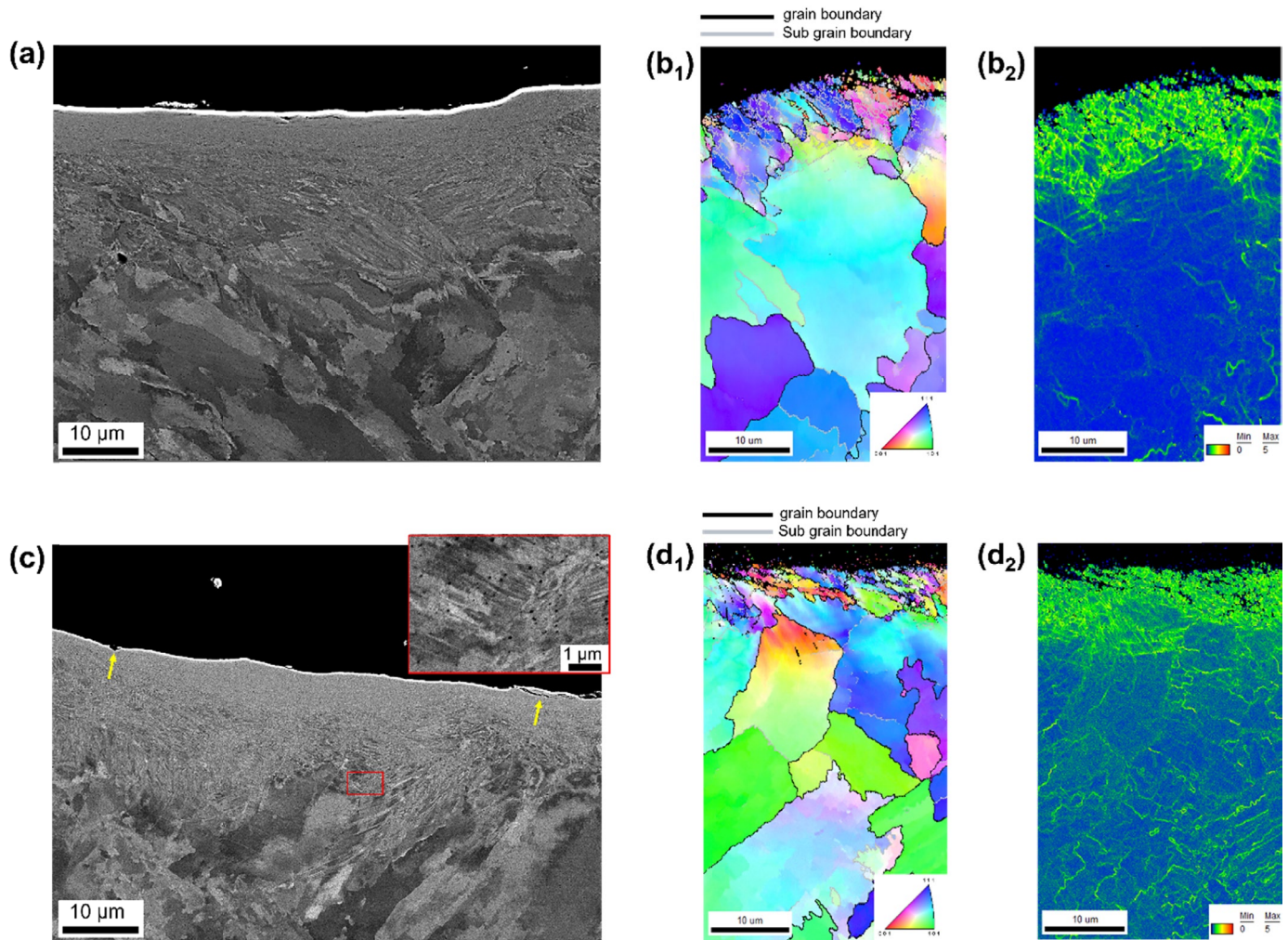


Fig. 5. The cross-sectional worn deformed microstructures; BSE-SEM images of (a) 5 N and (c) 15 N, and EBSD analysis results of (b) 5 N and (d) 15 N, and (a₁), (b₁) IPF maps and (a₂), (b₂) KAM maps

This HEA showed a much higher hardness value than conventional processed Cantor HEA due to its high dislocation density and in-situ oxide. As a result of the wear test, the 5 N condition showed a lower COF than 15 N and stable wear behavior, but the wear rate was higher at 5 N. Observation of microstructure after wear showed a finer worn microstructure in the case of 15 N, indicating a lower wear rate at higher loads due to surface reinforcement and self-lubrication by ultra-fine equiaxed grain.

Acknowledgments

This study was supported by National Research Foundation of Korea (NRF) grant funded by the Korea government (MEST) (No. 2022R1A2C3006964).

REFERENCES

- [1] E.P. George, W.A. Curtin, C.C. Tasan, *Acta Mater.* **188**, 435 (2020).
- [2] Y.F. Ye, Q. Wang, J. Lu, C.T. Liu, Y. Yang, *Mater. Today* **19**, 349 (2016).
- [3] B. Cantor, I.T.H. Chang, P. Knight, A.J.B. Vincent, *Sci. Eng. A* **375**, 231 (2004).
- [4] E.J. Pickering, N.G. Jones, *Int. Mater. Rev.* **61**, 183 (2016).
- [5] P. Asghari-Rad, N.T.-C. Nguyen, Y. Kim, A. Zargarani, P. Sathiamoorthi, H.S. Kim, *Mater. Lett.* **303**, 130503 (2021).
- [6] P.V. Satyanarayana, R. Sockalingam, P.K. Jena, K. Sivaprasad, K.G. Prashanth, *Metals* **9**, 992 (2019).
- [7] Y.-K. Kim, J.-H. Yu, H.S. Kim, K.-A. Lee, *Compos. Part B Eng.* **210**, 108638 (2021).
- [8] Y.-K. Kim, S. Yang, K.-A. Lee, *Addit. Manuf.* **36**, 101543 (2020).
- [10] W.H. Yu, S.L. Sing, C.K. Chua, C.N. Kuo, X.L. Tian, *Prog. Mater. Sci.* **104**, 330 (2019).
- [11] B. Song, Z. Wang, Q. Yan, Y. Zhang, J. Zhang, C. Cai, Q. Wei, Y. Shi, *Mater. Sci. Eng. A* **707**, 478 (2017).
- [12] Y.-K. Kim, S. Yang, K.-A. Lee, *Sci. Rep.* **10**, 8045 (2020).
- [13] Y.-K. Kim, M.-C. Kim, K.-A. Lee, *J. Mater. Sci. Technol.* **97**, 10 (2022).
- [14] Y.-K. Kim, J.-Y. Suh, K.-A. Lee, *Mater. Sci. Eng.* **796**, 140039 (2020).
- [15] S. Sonal, J. Lee, *Metals* **11**, 1980 (2021).
- [16] J. Wang, B. Zhang, Y. Yu, Z. Zhang, S. Zhu, X. Lou, Z. Wang, *Surf. Coat. Technol.* **384**, 125337 (2020).

- [17] J. Liu, A.C. To, *Addit. Manuf.* **16**, 58 (2017).
- [18] H. Zhang, M. Xu, P. Kumar, C. Li, W. Dai, Z. Liu, *Virtual Phys. Prototyp.* **16**, 125 (2021).
- [19] S. Mirzababaei, M. Ghayoor, R.P. Doyle, S. Pasebani, *Mater. Lett.* **284**, 129046 (2021).
- [20] J. Joseph, N. Haghadi, K. Shamlaye, P. Hodgson, M. Barnett, D. Fabijanic, *Wear* **428**, 32 (2019).
- [21] J.-E. Ahn, Y.-K. Kim, S.-H. Yoon, K.-A. Lee, *Metals Mater. Int.* **27**, 2406 (2021).
- [22] W.M. Rainforth, A.J. Leonard, C. Perrin, A. Bedolla-Jacuinde, Y. Wang, H. Jones, Q. Luo, *Tribol. Int.* **35**, 731 (2002).
- [23] C. Gao, D. Kuhlmann-Wilsdorf, D.D. Makel, *MRS Online Proceedings Library* **140**, 397 (1988).
- [24] A.D. Berman, W.A., Ducker, J.N. Israelachvili, *Langmuir* **12**, 4559 (1996).
- [25] J. Joseph, N. Haghadi, M. Annasamy, S. Kada, P.D. Hodgson, M.R. Barnett, D.M. Fabijani, *Scr. Mater.* **186**, 230 (2020).
- [26] S.K. Sambaraj, E.S. Sandeep, S.B. Chandrasekhar, S.K. Karak, *Mater. Res.* **19**, 175 (2016).
- [27] A. Zhang, J. Han, B. Su, P. Li, J. Meng, *Mater. Des.* **114**, 253 (2017).
- [28] G. Deng, A.K. Tieu, X. Lan, L. Su, L. Wang, Q. Zhu, H. Zhu, *Tribol. Int.* **144**, 106116 (2020).